JOURNAL OF PETROLEUM GEOMECHANICS
(JPG)

Original article

New Method for Modifying Winland Equation Using Well Log Data, Case Study of Kangan and Dalan Formations, the Central Persian Gulf

Shaghayegh Zarei Roodbaraki[1], Vahid Tavakoli[1*], Sogand Asadolahi Shad[1]

1- School of Geology, College of Science, University of Tehran, Tehran, Iran

Received: 16 April 2024; Accepted: 22 May 2024

DOI: 10.22107/jpg.2024.452868.1233

Keywords

Well Log Data,
Pore Throat Size,
Regression analysis,
Rock Typing,
Persian Gulf

Abstract

Efforts have been dedicated to correlating pore throat sizes with petrophysical and geological parameters. Log data is helpful in examining and analyzing the degree of pore type, the presence of clay minerals as well as porosity and the density of the reservoir. This study aims to establish a relationship between pore throat sizes and well log data through regression analysis. Well-logging data are routinely accessible and can be compared with the core data.The research uses mercury injection capillary pressure, core samples, and well log data from three wells within a field in the central Persian Gulf region. Equations were developed to link data from various well logs and their combinations to pore throat sizes in the reservoir. To address with challenges, core plugs were categorized into more homogeneous groups using Winland and flow zone indicator rock typing methods. The Winland method revealed that equations within each rock type exhibited low R^2 values due to significant porosity variations. Conversely, integrating data from all seven rock types yielded better fits as the diverse porosity values counterbalanced each other's effects. However, the flow zone indicator rock typing approach did not enhance results as it was designed for circular and cylindrical capillary tubes, making it less effective for developing complex equations in carbonate reservoirs. The findings underscore the significance of defining homogeneous units accurately, as this step is crucial for enhancing results and establishing robust relationships between pore throat sizes and well log data. By integrating data from various rock types and refining the approach to defining homogeneous units, the study demonstrates the potential for improving the accuracy and applicability of pore throat size predictions in carbonate reservoirs.

1. Introduction

Carbonate reservoirs contain half of the world's hydrocarbon in place [1]. Therefore, characterization of these reservoirs is essential in any formation evaluation process. Carbonates are more heterogeneous than sandstones, so determining their reservoir properties is more complicated. Most part of such complexity originates from their heterogeneous pore network and their connections. The pore throat sizes (PTS) and their distribution in these reservoirs have a major effect on fluid flow. So, determining PTS distribution (PTSD) is important to characterize any carbonate reservoir. Capillary pressure tests are routinely used for obtaining PTSD in reservoir rocks. In 1921 Washburn defined the equation between capillary pressure and pore throat size as equation 1:

$$Pc: -2Y\cos a/r_c \quad (1)$$

where Pc is capillary pressure (psi), Y is the surface tension of mercury (psi/microns), a is the contact angle of mercury with the pore surface (degree) (typically 140° for most rocks) and r is pore throat radius (microns). Mercury porosimetry that described by Purcell [2] is also useful, because it can be used in irregular shaped samples and takes less time to perform. Winland constructed some equations to relate PTS to permeability and porosity in different ranges of mercury saturation. Ultimately he pointed out that the best relationship between PTS, permeability

* **Corresponding Author: vtavakoli@ut.ac.ir**

and porosity is in 35 % of mercury saturation. Winland's equation published by Kolodzie [3] (Eq. 2).

$$\text{Log R35} = 0.732 + 0.588 \text{ Log K} - 0.864 \text{ Log phi} \quad (2)$$

where k is permeability (millidarcy) and phi is porosity (v/v). Pittman [4] extended Winland's work and introduced apex method. The apex method is based on a plot of mercury saturation over capillary pressure versus mercury saturation. The inflection point of the resulted hyperbola describes the modal class of the PTS. The Pittman's method confirmed the Winland's works. Rezaee [5] tried to make an equation for relating PTS to porosity and permeability for carbonates. Using multiple regression analysis, he pointed out that the best correlation for carbonates is in 50 % of mercury saturation.

All of these investigations are based on porosity and permeability of cores which are not available in many cases. In contrast, logs are accessible in all reservoir intervals and so constructing a relationship between logs and PTSD solves many reservoir problems. The aim of this study is to modifying Winland equation by wireline log data in Permian–Triassic carbonates of the central Persian Gulf Basin using single and multiple regression analysis. Winland and flow zone indicator (FZI) rock typing methods were used to divide the plug samples into more homogeneous groups and overcoming the natural complexity of the reservoir.

Until now, various studies have been conducted to investigate the reservoir quality, heterogeneities using the Winland method in the Kangan and Dalan formations in different fields [6, 7, 8, 9,]. However, none of the previous studies have investigated and modified the Winland equation using well log data. The relationships constructed again in any determined rock types. As this is one of the first studies in this field, despite some primary expectations about the relationships, all logs were used for constructing the equations.

2. Geological Setting and Stratigraphy

In Persian Gulf region (Fig. 1) Hercynian orogeny caused Carboniferous uplifting and subsequent erosion [10]. During Permian, the climate became warmer and arid [11]. Regressive clastic sediments deposited in Early Permian known as Faraghan Formation [10]. This formation consists of sandstones with minor amounts of siltstones, conglomerate and variegated sandy shales [12]. It is resting unconformably on older strata and has gradational contact with Dalan (Late Permian) carbonates [13]. At the end of Early Permian, marine transgression caused deposition of Dalan Formation. Existence of marine fossils in this formation indicates that it was deposited in an open marine conditions [14]. With depositional progradation and less subsidence, it shows a progressively restricted condition, resulted in evaporite deposition [10]. Dalan is lithologically subdivided into three members including lower carbonate, Nar evaporite and upper carbonate [15]. The upper Dalan has two reservoir units, K4 and K3 from bottom to top, respectively. A sea level regression has been confirmed in the end of Permian in Persian Gulf Basin [16, 17, 18] so the boundary between Dalan and Kangan (Early Triassic) is disconformable. In Triassic transgression, the Kangan Formation was deposited [19]. During Triassic, the climate changed between semi-arid and arid conditions [20]. Carbonates and evaporites of Early and Middle Triassic were deposited in shallow water environmental settings [21]. Kangan Formation consists of two reservoir units including K2 and K1. The upper limit of the formation is defined by the conformable contact of limestone and dolomites with shale and anhydrite of Dashtak Formation (Early-Mid Triassic) [22]. Table 1 shows the stratigraphy and general characteristics of the Kangan and Dalan formations studied in this research and the adjacent strata of the Persian Gulf basin.

3. Materials and Methods

To achieve the goals of this research, conventional logs including gamma ray (GR), sonic (DT), resistivity (Re), neutron (N) and density (RHO) were used for making equations. Log data were accessible from three wells, wells A, B and C. In every 0.1524 m of each well, one data was recorded. Other data consists of mercury injection capillary pressure (MICP) results from well A (29 samples), B (24 samples) and C (21 samples). These MICP samples were selected based on geological facies variations and porosity and permeability changes. Other routine core data was available from one well (well A). Porosity measured with Boyle's law from 1230 plug samples. Permeability of these samples measured with Darcy's law. Data of three wells were used to determine coefficients of Winland equation,

plotting logs versus each other and also versus PTS_{50}, making equations based on logs in MICP intervals. After that, by use of just well A data, new equations based on logs were constructed in cored interval. Then, 1230 plug samples were separated to more homogeneous groups. The thickness of the studied strata in wells B, A and C are 342.08, 470.64 and 503.36 m, respectively. Winland and FZI rock typing methods were used for defining more homogeneous reservoir units. It is also worth mentioning that in each step, logs were extracted in same depth of porosity and permeability by linear interpolation. Table 2 is related to the intervals and the number of data collected from all three studied wells.

Table 1. Stratigraphical column and main features of studied strata [18] -*The parts with stars are the formations and units studied in this research.

Group	Formation	Member	Unit	Age	Lithology	Environment
	Dashtak			Early-Mid Triassic	Shale and silty shale interbedded with dolomite and anhydrite	Shallow marine
Dehram	Kangan*		K1*	Early Triassic	Dolomitized limestone, dolomite and anhydrite	Shallow marine
			K2*			
	Dalan	Upper Dalan*	K3*	Late Permian	Limestone, dolomite, minor evaporate and sandstone	Restricted to open shelf
			K4*			
		Nar				
		Lower Dalan				
	Faraghan			Early Permian	Sandstone with minor variegated shale	Littoral, partly deltaic

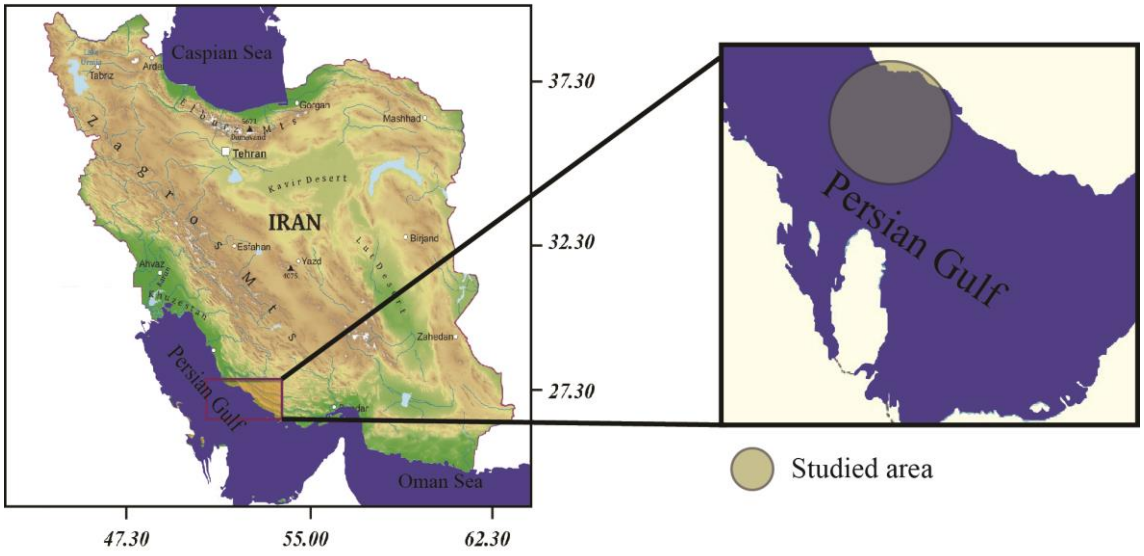

Fig. 1. Geographical position of the studied area in the Persian Gulf basin.

Table 2. Intervals taken from well-logging, core and mercury injection data of studied wells in Kangan and Dalan formations

	Well A	Well B	Well C
MICP Data	29 samples	24 samples	21 samples
Well Log Data	From 2891.028 to 3390.29 m	From 2772.298 to 3242.932 m	From 2632.428 to 3135.781 m
Core Data	From 2974.71 – to 3316.79 m	-	-

4. Result

4.1. Relationship of variables

The relationship between PTS (micrometer), permeability (mD) and porosity (%) in mercury saturation from 35 % to 75 % was evaluated. The value of 50 % was selected as best percentile of mercury saturation, while PTS_{45} had the highest coefficient of determination (R^2) between measured and evaluated saturations, because correspondence equation with R^2 of PTS_{50} had closest slope to one. PTS_{50} had the highest R^2 after PTS_{45}. Table 3 shows equations in different range of mercury saturation and their R^2 values. Achieved equation in PTS_{50} was used to obtain PTS of 1230 samples with measured core porosity and permeability.

Table 3. Equations and R^2 values between measured and evaluated saturations in different range of mercury injection

PTS = (a*LogK)+(b*Logphi)- c					
Percent of mercury saturation	a	b	c		R^2
35 %	0.28	0.70	-0.66	Y=0.65X+0.58	R^2: 0.74
40 %	0.27	0.89	-0.93	Y=0.65X+0.50	R^2: 0.75
45 %	0.29	0.67	-0.74	Y=0.68X+0.41	R^2: 0.77
50 %	0.27	0.94	-1.10	Y=0.69X+0.41	R^2: 0.75
55 %	0.27	0.66	-0.81	Y=0.55X+0.57	R^2: 0.71
60 %	0.27	0.88	-1.18	Y=0.57X+0.44	R^2: 0.73
65%	0.28	0.72	-1.03	Y=0.55X+0.42	R^2: 0.74
70%	0.29	0.72	-1.14	Y=0.52X+0.35	R^2: 0.72
75%	0.28	0.69	-1.18	Y=0.45X+0.33	R^2: 0.71

4.2. Equations Based on Log Data

In depth of MICP sample intervals, the best correlations between each two logs obtained by comparing R^2 values. Such correlation also calculated for various logs and PTS_{50}. The R^2 of density versus sonic showed the highest value (0.88) with negative correlation, neutron versus PTS_{50} had the highest R^2 value (0.09).

Combination of 1 to 5 logs were used to obtain PTS_{50} through simple and multiple regression analysis. First in MICP intervals, new equations were constructed. The results were compared with measured PTS_{50} in MICP tests. Table 4 presents highest R^2 for various logs. Range of R^2 is between 0 – 0.14. Then new equations were made in core intervals and the results were compared with PTS_{50} obtained from core analysis data. Table 5 presents highest R^2 for these correlations. It should be mentioned that the range of R^2 for all equations is between 0.00 – 0.27.

Table 4. Highest R^2 for various logs for correlating of PTS_{50} from MICP and log data

	1 log	2 logs	3 logs	4 logs
Highest R^2	Re	N, DT	N, RHO, Re	GR, RHO, N, DT

Table 5. Highest R^2 for correlating measured and calculated of PTS_{50} from core and log

	1 log	2 logs	3 logs	4 logs
Highest R^2	RHOB	DT and RHO	GR, DT, RHO	Re, RHO, N, DT
			DT, RHO, Re	

Reservoir properties differ widely in carbonates according to their place [23]. Rock typing reduce such heterogeneity with classifying the samples based on similar reservoir properties [24]. In this study, two well-known methods including Winland and FZI rock typing were selected for dividing the samples into more homogenous groups.

4.3. Winland Rock Typing

The Winland rock typing method categorizes data according to their PTS_{35} values. However, in this study, the data were grouped based on PTS_{50}, as the pore-throat size distribution at the 50th percentile of mercury saturation exhibited the highest correlation with reservoir characteristics. Seven rock types were distinguished. Table 6 shows the range of PTS_{50} in each rock type. New equations between log data and PTS_{50}were made for each rock type. The R^2 between log-predicted and Winland equation $PTS_{50}$was very low (0 – 0.23) for each rock type while integrating data from all seven rock types, showed high R^2 for all logs (0.73 – 0.95). Table 7 indicates the highest R^2 for various number of logs and their rock types. The seventh rock type has few samples, so it is not included in the tables.

Table 6. Values of PTS_{50} in determined rock types

Rock type	1	2	3	4	5	6	7
PTS_{50}	≤0.1	0.1- 0.2	0.2- 0.5	0.5- 1	1- 2	2- 5	5≤

Table 7. Highest R^2 for log-predicted and Winland equation PTS_{50} and their corresponding rock type

	1 log	RT	2 logs	RT	3 logs	RT	4 logs	RT	5 logs	RT
Highest R^2	DT	5	DT, GR	6	DT, GR, Re	6	GR, DT, N, Re	6	N, RHO, DT, GR, Re	6

4.4. FZI Rock Typing

In this method, values of FZI are calculated using three equations (Eq.3 to 5) [25]:

$$RQI = 0.0314\ (k/phi)^{1/2} \quad (3)$$

K: permeability (mD)
Phi: porosity (v/v)
RQI: Reservoir Quality Index (μm)

$$FZI = RQI/\ phi_z \quad (4)$$

Phi_z : normalized porosity (v/v)
FZI: Flow Zone Index (μm/ v/v)

$$Phi_z = phi/\ 1\text{-}phi \quad (5)$$

Data are separated based on FZI ranges. The limits of each group was determined using data distribution histogram in this study Fig. 2, Table 8. High tortuosity in carbonates causes low FZI values [25]. In each rock type, new equations were

made. Log-predicted and Winland equation PTS_{50} were compared. All of the equations showed low R^2 (0 – 0.28). Table 9 presents the logs that have highest R^2 and their corresponding rock type.

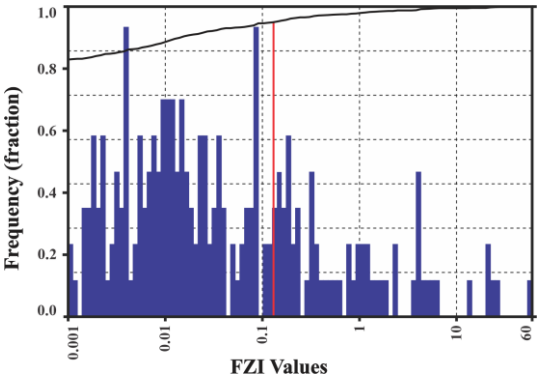

Fig. 2. Frequency diagram for FZI distribution in studied well

5. Discussion

Radioactive materials concentrate in shales, so the GR is mainly shale indicator [26]. Shales and clay minerals could mainly change the reservoir properties of the formations. Illite, for example, block the PTS or kaolinite fills the pores [27]. In carbonate reservoirs, the GR log as well as volume of shale and clay minerals are negligible (Fig. 3), so it is not expected that this log shows a good correlation with PTS.

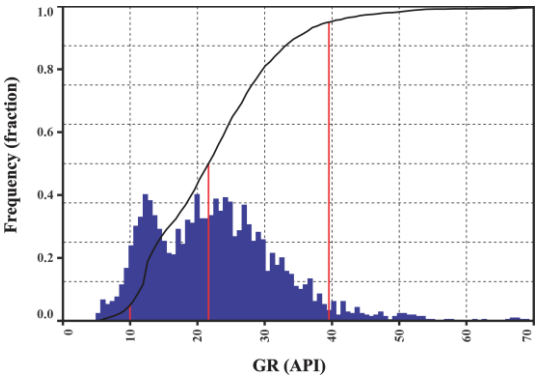

Fig. 3. GR distribution in Permian–Triassic carbonate strata of studied well in the central Persian Gulf

Table 8. The range of FZI in each rock type

Rock type	1	2	3	4
Range of FZI	>0.005	0.005- 0.05	0.05- 0.5	0.5<

Table 9. The logs that have highest R^2 and their corresponding rock types

	1 log	RT	2 logs	RT	3 logs	RT	4 logs	RT	5 logs	RT
Highest R^2	GR	3	GR, DT	3	N, DT, RHO	1	N, DT, RHO, Re	1	GR, N, DT, RHO, Re	1
			DT, RHO	1						

The correlation between this log and PTS showed low R^2. Sonic log measures interval transit time of a compressional sound wave [28]. It is applicable to determine connected porosity [23]. In the studied reservoir units, both interparticle and intercrystalline porosities are present, so it was expected that this log can relate to PTS, but constructed equations could not predict the PTSD of the samples. It is because of in many parts of the studied units, both connected and unconnected porosities are present. This increases the pore system heterogeneity and reduce the relevance of sonic log to PTS. Generally, there is no meaningful relationship between porosity and permeability in this reservoir (Fig. 4).

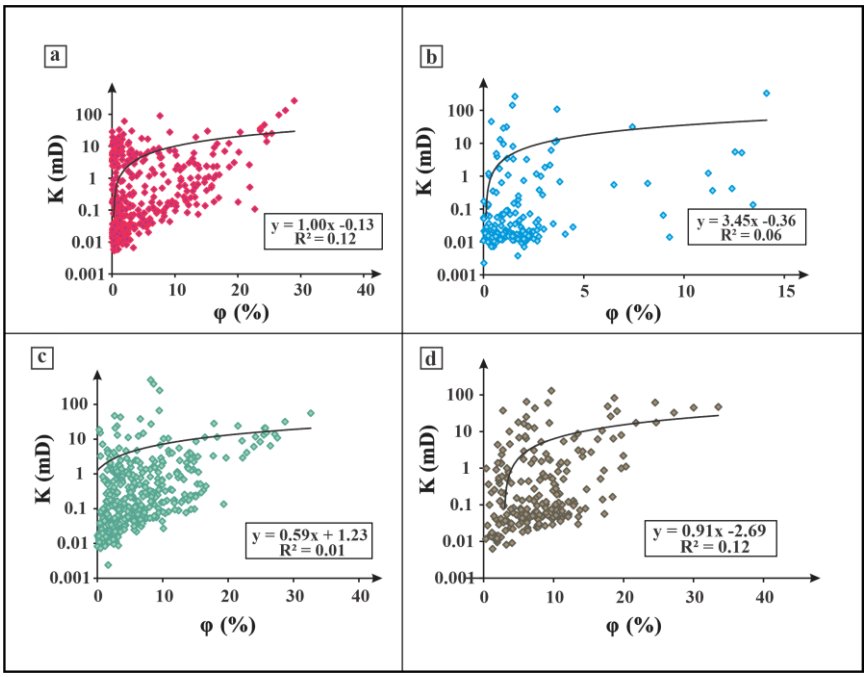

Fig. 4. Porosity – permeability plots of studied reservoir. K1 (a), K2 (b), K3 (c) and K4 units (d)

In neutron log, by increasing the amount of hydrogen in formation, count rates decrease [29]. The percentile of mercury saturation indicates the proportion of the space that contribute to fluid flow effectively [30]. In this way, pore size plus PTS is measured. In hydrocarbon intervals, water and hydrocarbon are situated in pore spaces and PTS. Both of components have hydrogen [28], so it was expected this tool relate to PTS. Equation for relating this log to PTS failed. In the studied reservoir, dissolution and dolomitization are two diagenetic processes that have important effects on reservoir quality [17]. Fabric selective dissolution during meteoric diagenesis generated moldic porosity [31]. Moldic pores have high porosity and low connectivity [32]. Dolomitization has less effect on porosity but it has high influence on permeability [33]. Degree of dolomitization has affected the reservoir quality, differently [17]. Overdolomitization causes to decrease reservoir quality [34]. These diagenetic processes in studied reservoir reduce the correlation of neutron response and PTSD. While high hydrogen concentration in separated molds correspond to low connectivity, there is various concentration in dolomitized parts according to degree of dolomitization. Fig. 5 shows diagenetic processes in studied reservoir.

Density log measures density of solid and fluid parts of formations [26]. Equation for relating this log to PTS had low R^2. The density log changes according to the bulk rock and fluid densities that are not change following the PTS.

The ability of transmit an electrical current in a rock is related to water in the pores. Rock's matrix and hydrocarbons are nonconductive. Salinity and temperature of water affect on this tool response [29]. Passage width has reverse relationship with resistivity [34]. New equation for this log failed, because different proportions of water and hydrocarbon are present in the pores.

For defining more homogeneous reservoir units, FZI and Winland rock typing methods were used. No meaningful results obtained from FZI rock typing method. The FZI rock typing is based on the concept of hydraulic unit radius (r_{mh}) that was developed for a circular, cylindrical capillary tube [25]. In heterogeneous pore system of carbonates, this concept is not appropriate for constructing such complicated relationships. In Winland rock typing, better results have been obtained using all data. This demonstrates that the way of defining more homogeneous reservoir units is significant. For calculating R^2, vertical distance between regression line and data points are calculated as residuals [36]. They could be

positive or negative according to their position with respect to the regression line. Deviations are really important for defining a good fit [37]. In Winland rock typing method, data points are scattered around the regression line in a way that negative and positive residuals have equal sum of squares. This is because in each rock type, in certain range of PTS, porosity can vary widely while in all seven rock types these porosities can neutralize the effect of each other.

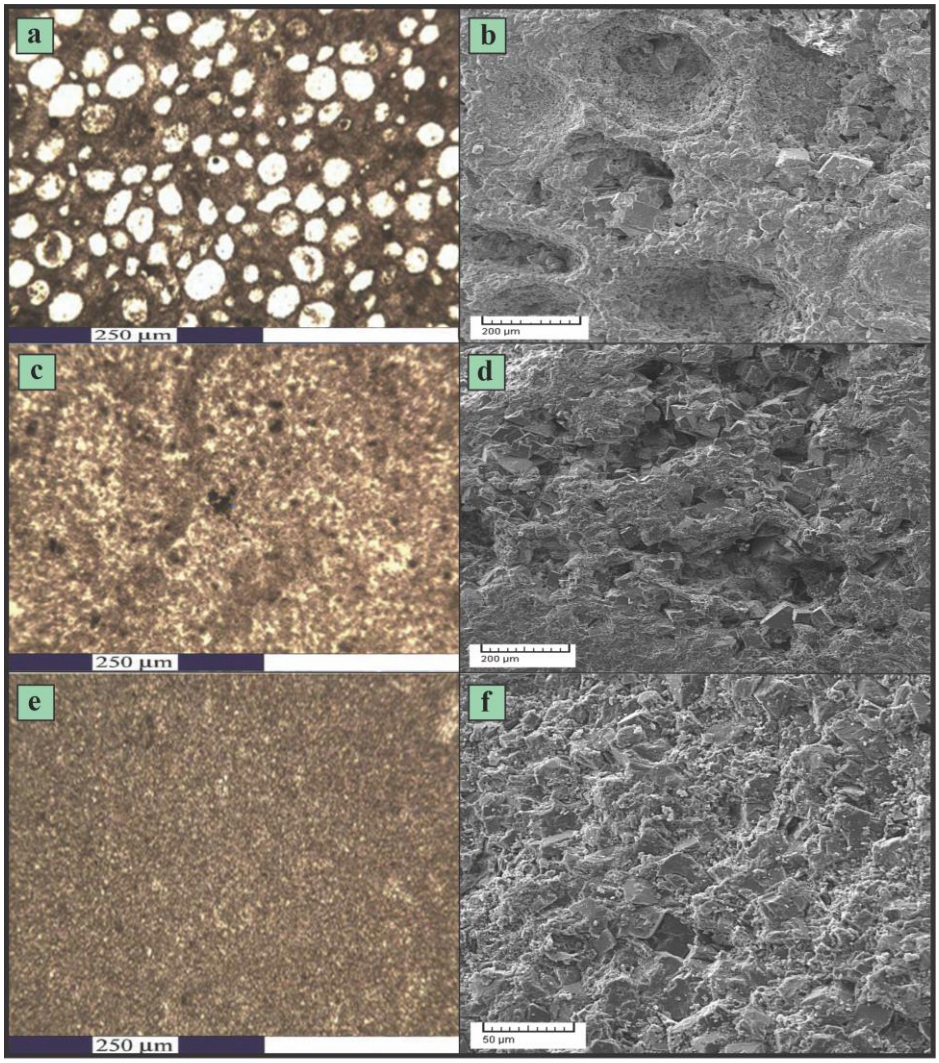

Fig. 5. Diagenetic processes in studied reservoir: moldic porosity resulted from dissolution (a, b), dolomitization (c, d), overdolomitization (e, f). Figures a, c and e obtained from thin sections in normal light. Figures b, d and f are obtained using SEM

Mean of core PTS of samples in each rock type and mean of PTS of new equations based on log data were calculated in each rock type. These two means change equal or in some cases nearly equal between different rock types. For example, in Table 10, difference between mean PTS of rock types in equations based on 5 logs are presented. The same change of PTS for both groups make a straight line in core versus log derived PTS in Winland method.

Table 10. Difference of mean PTS between determined rock types

Between these rock types	1. 2 μ	2. 3 μ	3. 4 μ	4.5 μ	5.6 μ	6.7 μ
Difference of mean PTS of core data	0.11 μ	0.17 μ	0.36 μ	0.64 μ	1.85 μ	3.3 μ
Difference of mean PTS of log data	0.12 μ	0.16 μ	0.36 μ	0.63 μ	1.79 μ	3.37 μ

6. Conclusions

The coefficients of Winland equation should be adjusted to the studied reservoir. In this study, by using petrophysical and well-logging data as well as identified rock types, the Winland standard equation has been modified. Well-logging data plays a crucial role in establishing a robust relationship between pore-throat size and rock types. By reducing reservoir heterogeneity, such data greatly aids in predicting pore-throat size in carbonate reservoirs. The best relationship between mercury saturation percentile and porosity-permeability data varies in various reservoirs. The PTS in 50 % of mercury saturation showed the best fit in Permian–Triassic Kangan and Dalan reservoirs in the central Persian Gulf Basin.

Equations for relating well logging data to PTS_{50} in whole intervals failed because of reservoir heterogeneity as well as tools mechanisms. Using Winland rock typing method, low R^2 was gained between calculated and measured PTS_{50} in each rock type. High R^2 value obtained for all data because in each rock type, in certain PTS, porosities vary widely but for all data, PTS scattering increase R^2 value significantly. FZI rock typing method could not make the results better because r_{mh} is the concept of this method. This concept is for a circular and cylindrical capillary tube. In complicated carbonates, this concept is not suitable.

7. References

[1] Ahr, W. M. (2008). Geology of carbonate reservoirs (1st ed.). Wiley.

[2] Purcell, W. R. (1949). Capillary pressures- their measurement using mercury and the calculation of permeability therefrom. American institute of mechanical engineers, petroleum transactions, pp. 39- 48.

[3] Kolodzie, S. Jr. (1980). Analysis of pore throat size and use of the Waxman- Smits equation to determine OOIP in Spindle field Colorado. Society of petroleum engineers, 55th annual fall technical conference paper 9382, pp.10.

[4] Pittman, E. D. (1992). Relationship of porosity and permeability to various parameters derived from mercury injection- capillary pressure curve for sandstone. AAPG Bulletin, 76, pp. 191- 198.

[5] Rezaee, M. R., Jafari, A., and Kazemzadeh, E. (2006). Relationships between permeability, porosity and pore throat size in carbonate rocks using Relationship of variables and neural networks. Journal of geophysics and engineering, pp. 370- 376.

[6] Tavakoli, V., Jamalian, A. (2019). Porosity evaluation in dolomitized Permain-Triassic strata of the Persian Gulf, insights into the porosity orgin of dolomite reservoirs, Journal of Petroleum Science and Engineering. 181(4):106191

[7] Tavakoli, V. (2021). Permeability's response to dolomization, clue from Permian-Triassic reservoirs of the central Persian Gulf. Marine and Petroleum Geology, 123: 104723.

[8] Mohsenipour, A., Soleimani, B., Zahmatkesh, I., Veisi, I. (2022). Determination of reservoir rock typing using integrating geological and petrophysical methods in one of the oil fields in south-west of Iran Carbonates and Evaporites. Springer, 37 (2): 31.

[9] Kakemem, U., Ghasemi, M., Adabi, M.H., Husinec, A., Mahmoudi, A., Anderskouv, K. (2023). Sedimentology and sequence stratigraphy of automated hydraulic flow units – The Permian Upper Dalan Formation, Persian Gulf. Marine and Petroleum Geology, 147:105965.

[10] Ghazban, F. (2009). Petroleum geology of the Persian Gulf (2th ed.). University of Tehran press.

[11] Insalaco, E., Virgone, A., Courme, B., Gaillot, J., Kamali, M., Moallemi, A., Lotfpour, M., and Monibi, S. (2006). Upper Dalan member and Kangan formation between the Zagros mountains and offshore Fars, Iran: depositional system, biostratigraphy and stratigraphic architecture. Geoarabia, 11, 2, pp. 75- 174.

[12] Szabo, F., and Kheradpir, A. (1978). Permian and Triassic stratigraphy, Zagros basin, south- west Iran. Journal of petroleum geology, 1, pp. 57- 82.

[13] Alavi, M. (2004). Regional stratigraphy of the Zagros fold- thrust belt of Iran and it'sproforeland evolution. American journal of science, 304, pp .1- 20

[14] Kalantari, A. (1994). Zagros lithostratigraphy and microfacies. National Iranian oil company, Geological lab, Zagros, 5, 2, pp. 277-288.

[15] Edgell, H. S. (1977). The Permian system as an oil and gas reservoir in Iran, Iraq and Arabia. Proc. Second Iranian geological symposium, Tehran, p.161-201.

[16] Tavakoli, V. (2015). Chemo stratigraphy of the Permian–Triassic strata of the offshore Persian Gulf, Iran.
In:Ramkumar.(Ed.),Chemostratigraphy:Concepts,Techniques, and Applications. Elsevier, pp. 373–393.

[17] Abdolmaleki, J., Tavakoli, V., and Asadi-Eskandar, A. (2016). Sedimentological and diagenetic controls on reservoir properties in the Permian–Triassic successions of western Persian Gulf, southern Iran. Journal of petroleum science and engineering 141, pp.90- 113.

[18] Tavakoli, V., Naderi-Khujin, M., and Seyedmehdi, Z. (2018). The end Permian regression in the western Tethys: sedimentological and geochemical evidence from off shore the Persian Gulf, Iran. Geo- Mar let, 38, pp. 179- 192.

[19] Tavakoli, V. (2017). Application of gamma deviation log (GDL) in sequence stratigraphy of carbonate strata, an example from offshore Persian Gulf, Iran. Journal of Petroleum Science and Engineering, 156, pp. 868-876.

[20] Read, J. F., and Horbury, A. D. (1993). Eustatic and tectonic controls on porosity evolution beneath sequence bounding unconformities and parasequence disconformities on carbonate platforms, in A. D. Horbury and A. G. Robinson, eds, diagenesis and basin development. AAPG studies in geology 36, pp. 155-198.

[21] Abdolmaleki, J., Tavakoli, V. (2016). Anachronistic facies in the early Triassic successions of the Persian Gulf andits paleoenvironmental reconstruction. Paleogeography, palaeoclimatology, paleoecology 446, pp. 213-224.

[22] Alsharhan, A. S., and Nairn, A. E. M. (1997). Sedimentary basins and petroleum geology of the middle east (1th ed.). Elsevier

[23] Kennedy, M. (2015). Practical petrophysics (1th ed.). Elsevier.

[24] Tavakoli, V. (2018). Geological core analysis: application to reservoir characterization (1th ed.). Springer.

[25] Amaefule, J. O., Altunbay, M., Tiab, D., Kersey, D. G., and Keelan, D. K. (1993). Enhanced reservoir description: using core and log data to identify hydraulic (flow) units and predict permeability in uncored intervals/ wells. Society of petroleum engineers, pp. 205- 218.

[26] Asquith, G., Krygowski, D. A., Hurley, N. F., and Henderson, S. (2004). Basic well log analysis (2th ed.). AAPG.

[27] Tucker, M. E. (2001). Sedimentary petrology: An introduction to the origin of sedimentary rocks (3th ed.). Black well science.

[28] Ellis, D. V., and Singer, J. M. (2008). Well logging for earth scientists (2th ed.). Springer.

[29] Serra, O. (1984). Fundamentals of well log interpretation (3th ed.). Elsevier.

[30] Swanson, B. F. (1977, September). Visualizing pores and non-wetting phase in porous rocks: Society of petroleum engineers, Annual fall technical conference, 6857, pp. 902-912.

[31] Esrafili-Dizaji, B., and Rahimpour-Bonab, H. (2009). Effects of depositional and diagenetic characteristics on carbonate reservoir quality: a case study from the south pars gas field in the Persian Gulf. Petroleum Geoscience, 15, pp. 325- 344.

[32] Lucia, F. J. (2007). Carbonate reservoir characterization (2th ed.). Springer.

[33] Warren, J. (2000). Dolomite: occurrence, evolution and economically important associations. Earth-Science Reviews 52, pp.1-81.

[34] Warren, J. K. (2006). Evaporites: sediments, resources and hydrocarbons (1th ed.). Springer.

[35] Durkan, C., and Welland, M. E. (1999). Size effects in the electrical resistivity of polycrystalline nanowires. The American physical society, 20, 61, pp. 4.

[36] Weisberg, S. (2005). Applied linear regression (3th ed.). Wiley inters science.

[37] Kleinbaum, D. G., Kupper, L. J., and Muller, K. E. (1987). Applied Relationship of variables and other multivariable methods (2th ed.). PWS – Kent publishing company.